Theoretical investigation of Rydberg states of He$_2$ using the R-matrix method

M. D. Epée Epée, O. Motapon, K. Chakrabarti & Jonathan Tennyson

Published online: 23 Dec 2023.

Submit your article to this journal ↗

Article views: 71

View related articles ↗

View Crossmark data ↗

Taylor & Francis
Taylor & Francis Group

OPEN ACCESS

Check for updates

Theoretical investigation of Rydberg states of He₂ using the R-matrix method

M. D. Epée Epée[a], O. Motapon[a,b], K. Chakrabarti[c] and Jonathan Tennyson [d,e]

[a]Department of Physics, Faculty of Science, University of Douala, Douala, Cameroon; [b]Faculty of Science, University of Maroua, Maroua, Cameroon; [c]Department of Mathematics, Scottish Church College, Kolkata, India; [d]Department of Physics and Astronomy, University College London, UK; [e]Laboratoire Ondes et Milieux Complexes, UMR 6294 CNRS and Université du Havre, Le Havre, France

ABSTRACT
Bound states of the He₂ molecule are determined from an electron-He$_2^+$ collision calculation using the R-matrix method. The calculations are performed at a moderately dense grid of 35 internuclear separations are used to characterise He₂ Rydberg states with $n \leq 7$. Potential energy curves for singlet $^1\Sigma_g^+$, $^1\Sigma_u^+$, $^1\Pi_g$, $^1\Pi_u$ and $^1\Delta_u$ and triplet $^3\Sigma_g^+$, $^3\Sigma_u^+$, $^3\Pi_g$, $^3\Pi_u$ and $^3\Delta_u$ Rydberg states of He₂ as well as effective quantum numbers as a function of internuclear separation are calculated. Based on the potential energy curves of A $^1\Sigma_g^+$, B $^1\Pi_g$, C $^1\Sigma_u^+$, F $^1\Pi_u$ and a $^3\Sigma_u^+$, b $^3\Pi_g$, c $^3\Sigma_g^+$, f $^3\Pi_u$, spectroscopic parameters ($T_e, D_e, R_e, \omega_e, \omega_e x_e, \alpha_e$ and B_e) of these states have been determined and compared with theoretical and experimental data available.
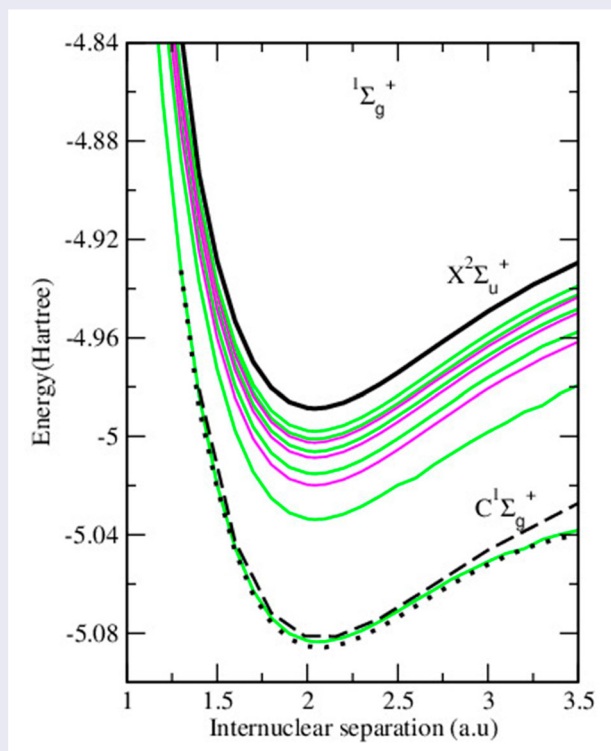
1. Introduction

He₂ was the first excimer (excited dimer) to be discovered and is an example of a Rydberg molecule [1]. Its ground state X $^1\Sigma_g^+$ is very shallow and the low-lying excited states are Rydberg states formed by a diffuse electron orbiting an He$_2^+$ core. The ground state of the He₂ molecule has been the subject of many works, particularly studies using high-level theory [2–7] for which it

CONTACT Jonathan Tennyson ✉ j.tennyson@ucl.ac.uk ▢ Department of Physics and Astronomy, University College London, Gower Street London, WC1E 6BT, UK

has become a benchmark system. Electronically excited states of He2 have been the subject of some experimental and theoretical studies [8–11] but have not been treated in detail with the exception of some states which have been studied in the context of particular problems such as the determination of cross-section for Penning and associative ionisation from the potential energy curves for the $^1\Sigma_g^+$ and $^1\Sigma_u^+$ autoionising states [12], electric dipole transition moments and Einstein spontaneous emission coefficients for X $^1\Sigma_g^+ \rightarrow$ A $^1\Sigma_u^+$ system [13].

The Rydberg states of the He2 molecule were first discovered in 1913 [14,15]. Since then, several calculations of bound states of He2 have been reported. Browne [16] computed the lowest $^1\Sigma_u^+$, $^3\Sigma_g^+$ and the first excited $^1\Sigma_g^+$ states of He2. A reasonable set of interatomic potential energy curves for a number of excited electronic

(Rydberg) states of He2 have been constructed using the Rydberg-Klein-Ress(RKR) procedure by Ginter and Battino [17]. The potential energy curve of the lowest singlet excited state A $^1\Sigma_u^+$ was calculated by Mukamel and Kaldor [18] and Komasa [13]. Cohen [8] obtained diabatic and adiabatic potential energy curves for the $^3\Sigma_{g,u}^+$, $^3\Pi_{g,u}$, $^3\Delta_g$ triplet states. Sunil et al. [19] used the Unitary Group multiconfiguration self-consistent field (MCSCF) procedure to calculate the potential curves of X $^1\Sigma_g^+$, C $^1\Sigma_g^+$, c $^3\Sigma_g^+$, A $^1\Sigma_u^+$, a $^3\Sigma_u^+$. Konowalow and Lengsfield [20] obtained from second-order configuration interaction calculations, the potential energy curves of $^3\Sigma_u^+$ states of He2 which correspond to the interactions of He($1s^2$ ^1S) and He($1s2s$ ^3S), and He($1s2s$ ^3S) with He($1s2s$ ^3S). They also produced vibrational energy levels and their spacing for the a $^3\Sigma_u^+$ of ^{4}He2. The properties

Table 1. Quantum defects (μ) and vertical excitation energies (in eV) of singlet $^1\Sigma_g^+$, $^1\Sigma_u^+$ and $^1\Pi_g$ Rydberg states of He2 molecule at $R = 2.00$ a$_0$ relative to a $^3\Sigma_u^+$.

		Vertical excitation energies			
State	μ	This work	Experiment[a]	Yarkony[b]	Sunil[c]
$^1\Sigma_u^+$					
2sσ A $^1\Sigma_u^+$	0.134525	0.296107	0.287264	0.288182	0.290937
3sσ D $^1\Sigma_u^+$	0.120322	2.574338	2.608188		
3dσ F $^1\Sigma_u^+$	0.040877	2.668197	2.698446		
4sσ H $^1\Sigma_u^+$	0.117323	3.308933	3.459442		
4dσ J $^1\Sigma_u^+$	0.043545	3.362413	3.493041		
5sσ $^1\Sigma_u^+$	0.114323	3.632030			
5dσ M $^1\Sigma_u^+$	0.044970	3.664469	3.806217		
5gσ $^1\Sigma_u^+$	−0.005281	3.666536			
6sσ $^1\Sigma_u^+$	0.113172	3.814288			
6dσ $^1\Sigma_u^+$	0.045668	3.821931			
6gσ $^1\Sigma_u^+$	−0.005343	3.830332			
$^1\Sigma_g^+$					
2pσ C $^1\Sigma_g^+$	−0.298769	1.624527	1.657254	1.660902	1.635336
3pσ $^1\Sigma_g^+$	−0.330391	2.976254			
4fσ $^1\Sigma_g^+$	−0.004093	3.355930			
4pσ $^1\Sigma_g^+$	−0.342025	3.482441			
5fσ $^1\Sigma_g^+$	−0.005326	3.661572			
5pσ $^1\Sigma_g^+$	−0.347717	3.728662			
6hσ $^1\Sigma_g^+$	0.002658	3.826335			
6fσ $^1\Sigma_g^+$	−0.006084	3.827513			
6pσ $^1\Sigma_g^+$	−0.350884	3.867249			
7hσ $^1\Sigma_g^+$	0.002213	3.926813			
7fσ $^1\Sigma_g^+$	−0.006575	3.927557			
7pσ $^1\Sigma_g^+$	−0.352849	3.952962			
$^1\Pi_g$					
2pπ B $^1\Pi_g$	0.017437	0.743615	0.727273	0.770405	
3pπ E $^1\Pi_g$	0.021856	2.679953	2.710597		
4fπ $^1\Pi_g$	−0.010316	3.357751			
4pπ I $^1\Pi_g$	0.019259	3.352443	3.498495		
5pπ L $^1\Pi_g$	0.019483	3.656336	3.811920		
5fπ $^1\Pi_g$	−0.009377	3.665412			
6pπ P $^1\Pi_g$	0.019784	3.818259	3.981278		
6fπ $^1\Pi_g$	−0.009334	3.827151			
7pπ R $^1\Pi_g$	0.020135	3.929327	4.083314		
7fπ $^1\Pi_g$	−0.010463	3.925274			

[a]Experiment from Huber and Herzberg [9].
[b]Yarkony [21], Vertical excitation energies calculated at $R = 2.00$ a$_0$.
[c]Sunil et al. [19],Vertical excitation energies calculated at $R = 1.984$ a$_0$

Table 2. Quantum defects (μ) and vertical excitation energies (in eV) of $^1\Pi_u$ and $^1\Delta_u$ singlet Rydberg states of He_2 molecule at $R = 2.00$ a$_0$ relative to a $^3\Sigma_u^+$.

State	μ	Vertical excitation energies	
		This work	Experiment[a]
$^1\Pi_u$			
$3d\pi$ F $^1\Pi_u$	0.022715	2.668037	2.718035
$4d\pi$ J $^1\Pi_u$	0.024087	3.443289	3.501471
$5g\pi$ $^1\Pi_u$	−0.001593	3.754615	
$5d\pi$ M $^1\Pi_u$	0.025023	3.760834	3.811176
$6g\pi$ $^1\Pi_u$	−0.001551	3.823327	
$6d\pi$ $^1\Pi_u$	0.025486	3.826993	
$7g\pi$ $^1\Pi_u$	−0.001539	3.924860	
$7d\pi$ $^1\Pi_u$	0.025732	3.927187	
$^1\Delta_u$			
$4d\delta$ $^1\Delta_u$	0.001478	3.353971	
$5d\delta$ $^1\Delta_u$	0.001506	3.660178	
$6d\delta$ $^1\Delta_u$	0.001512	3.826596	
$7d\delta$ $^1\Delta_u$	0.001638	3.926940	
$8d\delta$ $^1\Delta_u$	0.001756	3.992060	
$9d\delta$ $^1\Delta_u$	0.001778	4.046704	
$10d\delta$ $^1\Delta_u$	0.003063	4.068302	

[a] Experiment from Huber and Herzberg [9].

of the excited states of He_2 have also been calculated by Yarkony [21]. Energies, effective quantum number and quantum defect for $He_2(1\sigma_g^2 1\sigma_u ns, nd\sigma$ and $ng\sigma)$ bound state for $^3\Sigma_u^+$ state were performed using the R-matrix technique with a (4s,2p,2d) Slater basis at full CI levels [22]. As indicated by Guberman [23], the $^3\Sigma_g^+$ and $^1\Sigma_g^+$ states provide the main routes for dissociative recombination of He_2^+, but other diabatic states of He_2, such as $^3\Pi_u$, $^1\Pi_u$, $^3\Sigma_u^+$ and $^1\Sigma_u^+$ are also possible routes. In a previous study [24], we used the R-matrix method to characterise these dissociative resonant states of He_2 and included consideration of these when they become bound at large internuclear separation. However, we did not study the Rydberg states of He_2 which, amongst other things, play an important role in the dissociative recombination process.

The use of electron–molecular ion scattering wavefunctions has proved to be a powerful method of characterising Rydberg states which have been shown to be

Table 3. Quantum defect (μ) and vertical excitation energies (in eV) of triplet $^3\Sigma_u^+$, $^3\Sigma_g^+$ and $^3\Pi_g$ Rydberg states of He_2 molecule at $R = 2.00$ a$_0$ relative to a $^3\Sigma_u^+$.

T_e State	μ	Vertical excitation energies			
		This work	Experiment[a]	Yarkony[b]	Sunil[c]
$^3\Sigma_u^+$					
$2s\sigma$ a $^3\Sigma_u^+$	0.200152	0.000000	0.000000	0.000000	0.000000
$3s\sigma$ d $^3\Sigma_u^+$	0.187115	2.495503	2.533056		
$3d\sigma$ f $^3\Sigma_u^+$	0.053893	2.650625	2.682577		
$4s\sigma$ h $^3\Sigma_u^+$	0.180755	3.279669	3.327154		
$4d\sigma$ j $^3\Sigma_u^+$	0.061896	3.369378	3.381581		
$5s\sigma$ k $^3\Sigma_u^+$	0.178270	3.624166	3.676037		
$5d\sigma$ m $^3\Sigma_u^+$	0.065866	3.650884	3.803985		
$5g\sigma$ $^3\Sigma_u^+$	−0.005281	3.663642			
$6s\sigma$ o $^3\Sigma_u^+$	0.177186	3.799256	3.961564		
$6d\sigma$ q $^3\Sigma_u^+$	0.067958	3.830272	3.976319		
$6g\sigma$ $^3\Sigma_u^+$	−0.005342	3.829979			
$^3\Sigma_g^+$					
$2p\sigma$ c $^3\Sigma_g^+$	−0.191187	1.376796	1.364411	1.366949	1.354957
$3p\sigma$ $^3\Sigma_g^+$	−0.212333	2.894609	2.934134		
$4f\sigma$ $^3\Sigma_g^+$	−0.004064	3.369205			
$4p\sigma$ g $^3\Sigma_g^+$	−0.223426	3.448137	3.494776		
$5f\sigma$ $^3\Sigma_g^+$	−0.005282	3.655231			
$5p\sigma$ k' $^3\Sigma_g^+$	−0.228528	3.712221	3.761708		
$6h\sigma$ $^3\Sigma_g^+$	0.003036	3.829970			
$6f\sigma$ $^3\Sigma_g^+$	−0.006031	3.826191			
$6p\sigma$ n $^3\Sigma_g^+$	−0.231294	3.847748			
$7h\sigma$ $^3\Sigma_g^+$	0.002601	3.920462			
$7f\sigma$ $^3\Sigma_g^+$	−0.006515	3.921235			
$7p\sigma$ p' $^3\Sigma_g^+$	−0.232960	3.938174	4.013637		
$^3\Pi_g$					
$2p\pi$ b $^3\Pi_g$	0.022473	0.606582	0.593497		
$3p\pi$ e $^3\Pi_g$	0.026892	2.587384	2.671791		
$4p\pi$ i $^3\Pi_g$	0.023295	3.343095	3.377490		
$4f\pi$ $^3\Pi_g$	−0.005280	3.348063			
$5p\pi$ l $^3\Pi_g$	0.024519	3.667801	3.699097		
$5f\pi$ $^3\Pi_g$	−0.004341	3.667765			
$6p\pi$ p $^3\Pi_g$	0.024820	3.791973	3.872298		
$6f\pi$ $^3\Pi_g$	−0.004298	3.791756			

[a] Experiment from Huber and Herzberg [9].
[b] Yarkony [21], Vertical excitation energies calculated at $R = 2.00$ a$_0$.
[c] Sunil et al. [19], Vertical excitation energies calculated at $R = 1.984$ a$_0$.

able to treat many more of the diffuse states more reliably than standard quantum chemistry methods, see studies of the Rydberg states of HeH [25] and N_2 [26]. The purpose of the present study is to provide a consistent, comprehensive set of data for He_2 Rydberg states. These results can be used for the calculation of cross-section and rate coefficients of dissociative recombination and related competitive processes, as well as interpretation of Rydberg state spectra.

2. Calculations

2.1. Method

Details of the calculations are already presented in our earlier work [24], so we only focus on the essentials. The R-matrix method [27] as implemented in the UKRMol codes [28] starts by dividing the configuration space into two distinct regions [29] by a sphere, here of radius 12 a_0, centred at the centre-of-mass of the He_2^+ molecule. This encloses the wave function of the 3-electron target He_2^+ ion. In the inner region, the wave functions for the target + scattering electron system (He_2^+ + electron) is given by:

$$\Psi_k^{N+1}(x_1, \ldots, x_{N+1})$$
$$= \mathcal{A} \sum_{ij} a_{ijk} \phi_i^N(x_1, \ldots, x_N) u_{ij}(x_{N+1})$$
$$+ \sum_i b_{ik} \chi_i^{N+1}(x_1, \ldots, x_{N+1}), \tag{1}$$

Table 4. Quantum defect (μ) and vertical excitation energies (in eV) of $^3\Pi_u$ and $^3\Delta_u$ singlet Rydberg states of He_2 molecule at $R = 2.00\ a_0$ relative to a $^3\Sigma_u^+$.

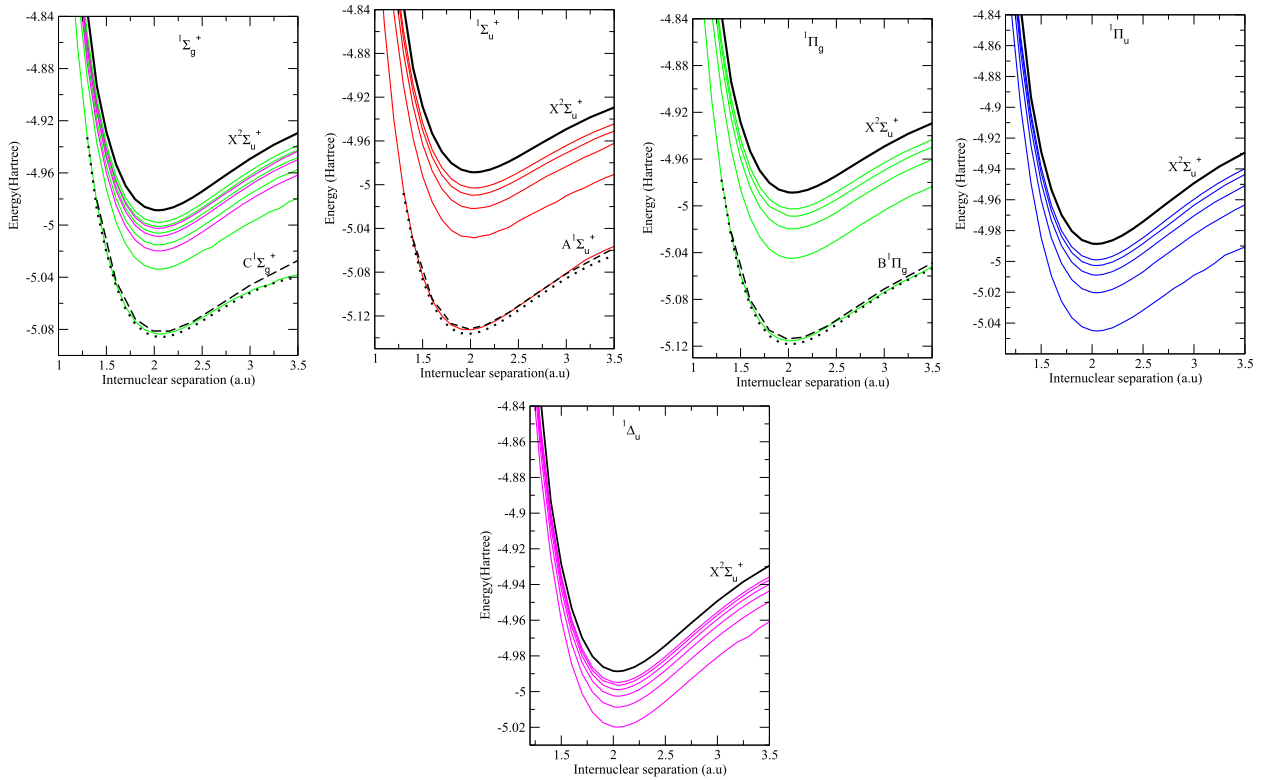|		Vertical excitation energies	
State	μ	This work	Experiment[a]
$^3\Pi_u$			
$3d\pi\ f\ ^3\Pi_u$	0.032575	2.660323	2.706381
$4d\pi\ j\ ^3\Pi_u$	0.038570	3.338344	3.391376
$5g\pi\ ^3\Pi_u$	−0.001493	3.754523	
$5d\pi\ m\ ^3\Pi_u$	0.041392	3.754469	3.809936
$6g\pi\ ^3\Pi_u$	−0.001550	3.826781	
$6d\pi\ q\ ^3\Pi_u$	0.042880	3.816585	
$7g\pi\ ^3\Pi_u$	−0.001539	3.928702	
$7d\pi\ ^3\Pi_u$	0.043742	3.917011	
$^3\Delta_u$			
$4d\delta\ ^3\Delta_u$	0.000547	3.347656	
$5d\delta\ ^3\Delta_u$	0.001520	3.653858	
$6d\delta\ ^3\Delta_u$	0.001553	3.827402	
$7d\delta\ ^3\Delta_u$	0.001671	3.926174	
$8d\delta\ ^3\Delta_u$	0.001695	3.985738	
$9d\delta\ ^3\Delta_u$	0.001744	4.038149	

[a]Experiment from Huber and Herzberg [9].

Figure 1. Potential energy curves of the lowest singlet $^1\Sigma_g^+$ ($np\sigma$ (green),$nf\sigma$ (magenta)), $^1\Sigma_u^+$ ($ns\sigma$), $^1\Pi_g$ ($np\pi$), $^1\Pi_u$ ($nd\pi$) and $^1\Delta_u$ ($nd\delta$) states of He_2. The symmetry of each set of bound states is indicated in the panel. Continuous curves: present calculation. Black dotted and dashed curves in the $^1\Sigma_g^+$, $^1\Sigma_u^+$ and $^1\Pi_g$ figures: Yarkony [21] and Wasilewski *et al.* [35] respectively. In each panel, the top black thick curve is the ground X $^2\Sigma_u^+$ state of He_2^+.

where $\mathcal{A}$ is the anti-symmetrisation operator, u_{ij} are known as continuum orbitals, x_i are the spatial and spin coordinates of electron i, ϕ_i^N is the wave functions of the ith target state and χ_i are two-centre L^2 functions constructed as products of target occupied and virtual molecular orbitals. The variational coefficients a_{ijk} and b_{ik} are determined by diagonalising the Hamiltonian matrix [30]. No allowance is made for relativistic effects such as spin-orbit coupling.

2.2. Target calculations

It is known that the basis sets play an important role in the quality of the calculation. For the present work, we use the cc-pVTZ Gaussian basis set for He_2^+, which include polarisation functions. An initial set of molecular orbitals was obtained by performing self-consistent field (SCF) calculations for the $X^2\Sigma_u^+$ state of He_2^+, although in practice the choice of orbitals is not important in a full configuration interaction (FCI) calculation. The two lowest He_2^+ states, $X^2\Sigma_u^+$ and $A^2\Sigma_g^+$, were included in the close-coupling expansion of the trial wave function of the

scattering system; the other target states lie too high in energy to contribute significantly at the energies considered here. Each target state was represented by an FCI wave function. Our FCI calculations performed for the ground state $X^2\Sigma_u^+$ and the first excited state $A^2\Sigma_g^+$ of the He_2^+ molecular ion were in very close agreement with high accuracy calculations [24].

2.3. Scattering calculations

The scattering calculations performed in this work were carried out using the fixed-nuclei formulation of R-matrix theory. This scattering calculations used a two-term close-coupling expansion based on the FCI representation of the He_2^+ $X^2\Sigma_u^+$ and $A^2\Sigma_g^+$ target states. To represent the continuum Gaussian-Type Orbitals (GTOs) were placed at the centre of the R-matrix sphere; the functions involved partial waves up to $\ell = 4$ (g functions) and were taken from Faure et $al.$ [31]. The FCI L^2 functions were generated by allowing all 4 electrons to occupy any target orbital subject only to the constraints of total symmetry. These L^2 terms relax the orthogonality
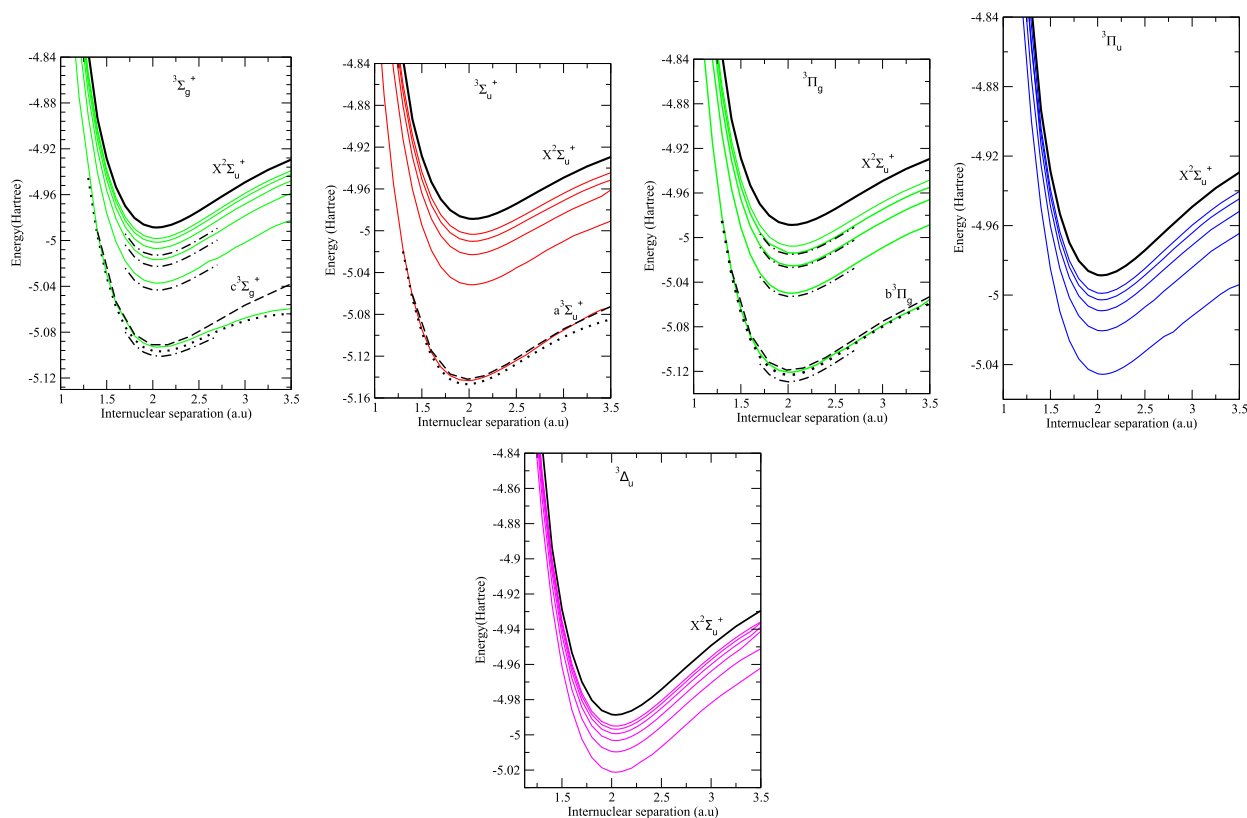

Figure 2. Potential energy curves of the lowest triplet $^3\Sigma_g^+(np\sigma)$, $^3\Sigma_u^+(ns\sigma)$, $^3\Pi_g(np\pi)$, $^3\Pi_u(nd\pi)$ and $^3\Delta_u(nd\delta)$ states of He$_2$. The symmetry of each set of bound states is indicated in the panel. Continuous curves: present calculation. Black dotted and dashed curves in the $^3\Sigma_g^+$, $^3\Sigma_u^+$ and $^3\Pi_g$ figures; Yarkony [21] and Wasilewski et $al.$ [35]. In each panel, the top black thick curve is the ground X $^2\Sigma_u^+$ state of He$_2^+$.

constraint between the continuum and target functions, allow for high ℓ behaviour of the scattered electron in the region of the target and for short-range polarisation effects. At long-range (in the outer region) polarisation is at least partially allowed for by the dipole coupling of the two electronic states.

Calculations were performed for singlet and triple spin symmetries and using C_{2v} point group symmetry. Our results have been recast using standard linear molecule symmetry notation.

2.4. Bound states

After solving the inner region problem, the solutions were used to build the R-matrix on the boundary. To use a scattering calculation as the basis for bound state finding requires adaptation of the standard R-matrix method and in particular the calculation of wavefunctions in the outer region. For a bound state, these functions must asymptotically tend to zero and match inner region functions on the R-matrix boundary. We used the algorithm
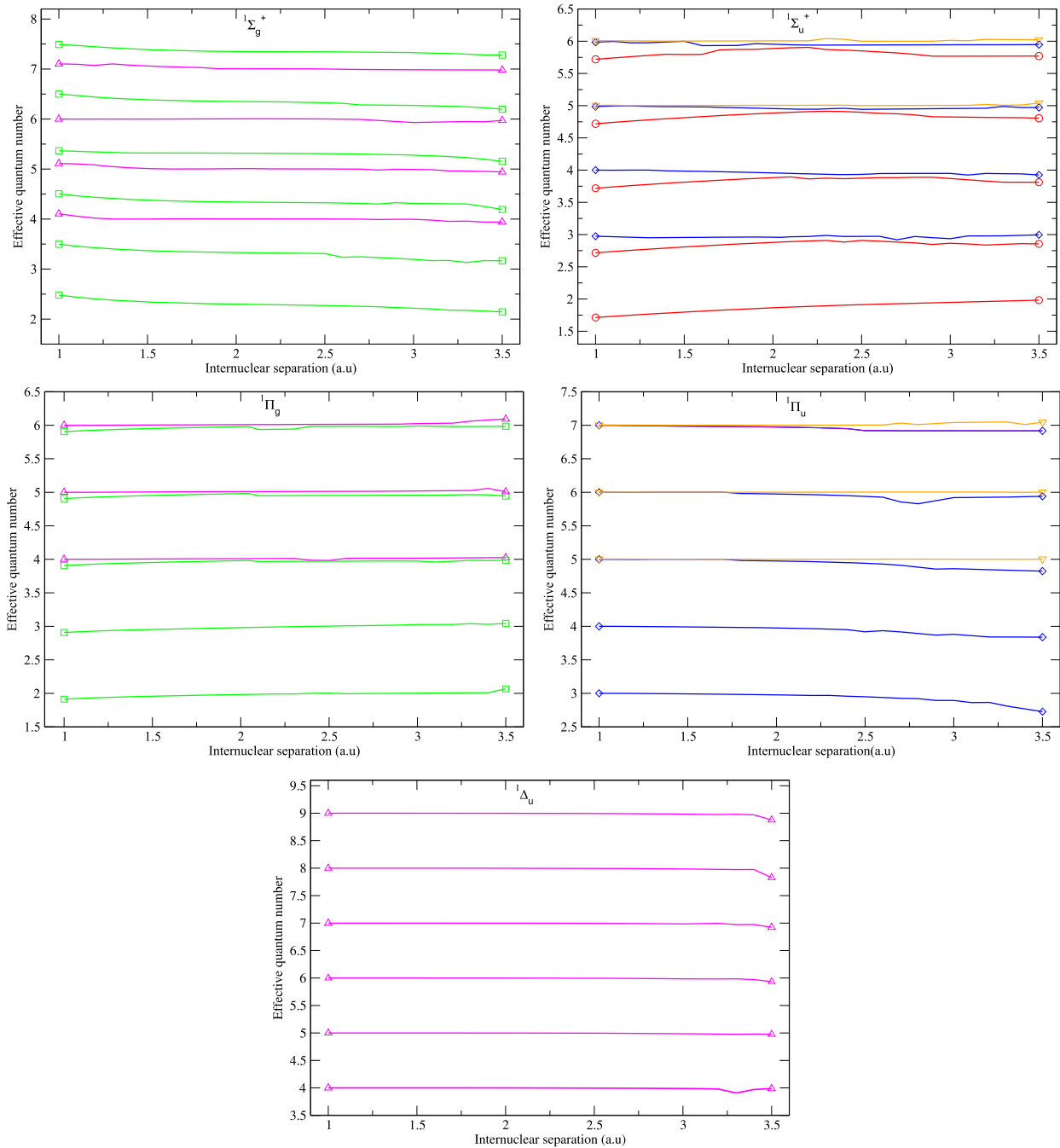

Figure 3. Effective quantum number of He$_2$ singlet bound states $^1\Sigma_g^+(np\sigma, nf\sigma)$, $^1\Sigma_u^+$ ($ns\sigma, nd\sigma, ng\sigma$), $^1\Pi_g$ ($np\pi, nf\pi$), $^1\Pi_u$ ($nd\pi$, $ng\pi$) and $^1\Delta_u(nd\delta)$ as function of the bond length. The l character of each state is indicated by the following symbols: circle : s-state, diamond : p-state, square : d-state triangle: f-state.

of Sarpal *et al.* [25] to find such states. The procedure uses an asymptotic expansion due to Gailitis [32] to determine the wavefunction at some intermediate distance, here of 30.1 a_0. From here the wavefunction was integrated inwards using an improved Runge-Kutta-Nystrom integration procedure, as implemented by Zhang *et al.* [33]; the bound state searching algorithm uses a nonlinear, quantum defect-based grid [34].

3. Results and discussion

In this section, we present our results of bound states of He_2 for those symmetries which couple to partial waves with $\ell \leq 2$, namely singlet $^1\Sigma_g^+$, $^1\Sigma_u^+$, $^1\Pi_u$, $^1\Pi_g$, $^1\Delta_u$ and triplet $^3\Sigma_g^+$, $^3\Sigma_u^+$, $^3\Pi_g$, $^3\Pi_u$, $^3\Delta_u$ symmetries. Tables 1–4 give quantum defects and vertical excitation energies for Rydberg series converging to the X $^2\Sigma_u^+$ ground states of
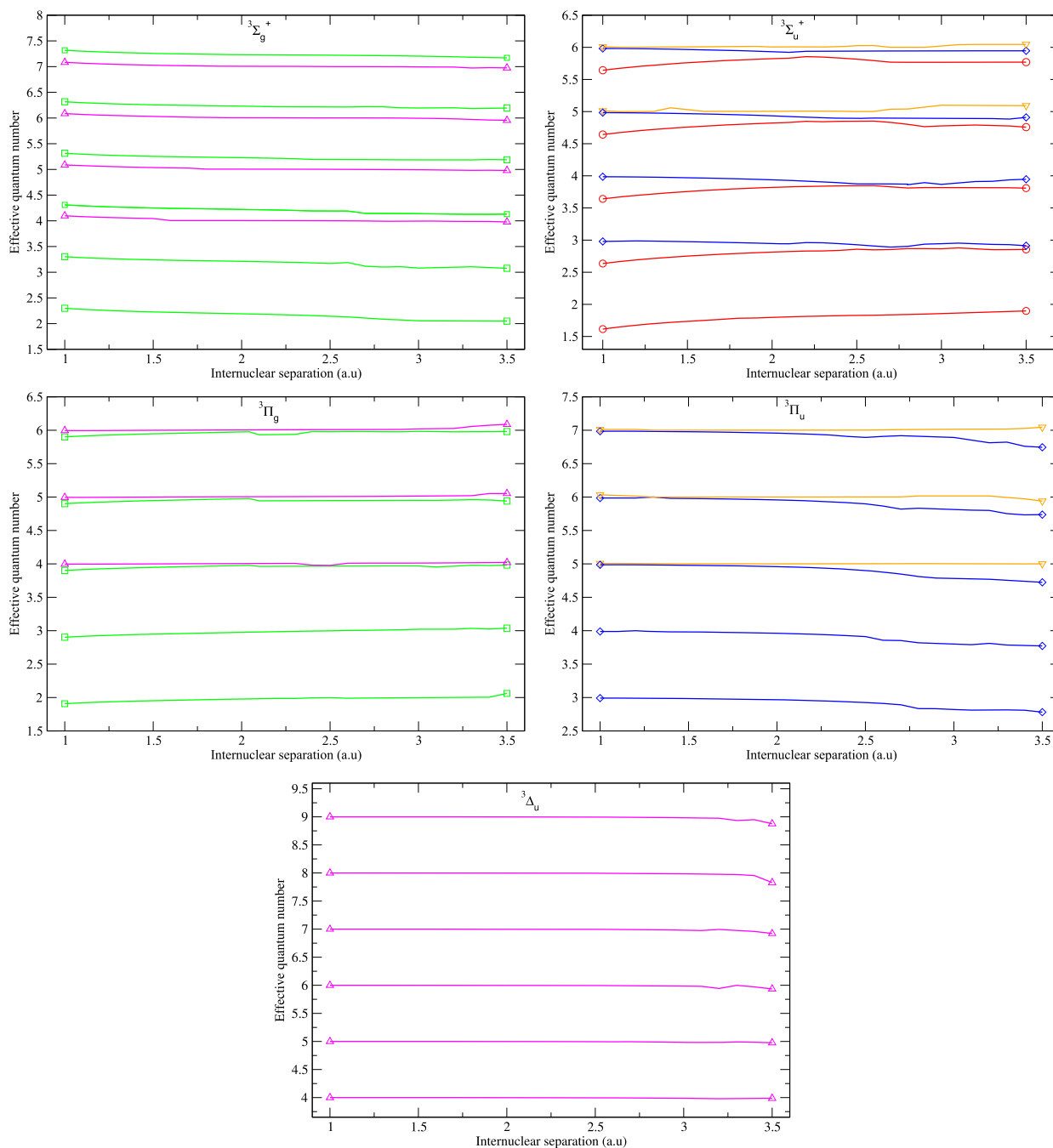

Figure 4. Effective quantum number of He_2 singlet bound states $^3\Sigma_g^+(np\sigma, nf\sigma)$, $^3\Sigma_u^+(ns\sigma, nd\sigma, ng\sigma)$, $^3\Pi_g(np\pi, nf\pi)$, $^3\Pi_u(nd\pi, ng\pi)$ and $^3\Delta_u(nf\delta)$ as function of the bond length. The *l* character of each state is indicated by the following symbols:circle : s-state, diamond : p-state, square : d-state triangle: f-state.

the ion. Vertical excitation energies (the energy difference between the ground and an excited state as taken at the ground state equilibrium bondlength) for some of the lower lying states of He$_2$ are compared with experimental data of Huber and Herzberg [9] and other calculations. Our excitation energies are in good agreement and are within 0.16 eV of the experiments and the other calculations present in the table. We also present in Tables 1–4 our calculated quantum defects for these states for the fixed internuclear separation of 2.00 a_0.

To obtain potential energy curves for Rydberg states of He$_2$ our calculations were repeated for 35 bondlengths in the range $R = 1.0$ to 3.5. Figures 1 and 2 display, respectively, singlet $^1\Sigma_g^+$, $^1\Sigma_u^+$, $^1\Pi_u$, $^1\Pi_g$, $^1\Delta_u$ and triplet $^3\Sigma_g^+$, $^3\Sigma_u^+$, $^3\Pi_g$, $^3\Pi_u$, $^3\Delta_u$ Rydberg states of He$_2$ as a function of bond separation. All curves couple to the ground state of the ion X $^2\Sigma_u^+$ and are more or less parallel to this state, as might be expected for Rydberg states. From Figures 1 and 2, it is seen that our curves are in satisfactory agreement with the multi-configuration self-consistent field (MCSCF) calculations of Sunil *et al.* [19]

Table 5. Spectroscopic constants of singlet A $^1\Sigma_u^+$, C $^1\Sigma_g^+$, B $^1\Pi_g$ and F $^1\Pi_u$ and triplet a $^3\Sigma_u^+$, c $^3\Sigma_g^+$, b $^3\Pi_g$ and f $^3\Pi_u$ Rydberg states of He$_2$.

State	R_e(Å)	T_e (cm^{-1})	D_e (cm^{-1})	ω_e(cm^{-1})	$\omega_e x_e$(cm^{-1})	B_e(cm^{-1})	α_e(cm^{-1})
a $^3\Sigma_u^+$							
This work.	1.0466	144 192	15151.7230	1787.862	42.3944	7.69135	0.2510
CEPA[a]	1.0483		15057.0388	1816.00	34.50		
MCSCF[b]	1.0504		15312.3615	1794.50	36.40	7.6342	0.2291
MCSCF/CI[c]	1.0500	143 807	15751	1808.2			
Experiment[d]	1.0457	144 048	15805.5188	1808.56	38.80	7.7036	0.2281
Experiment[e]	1.0454			1808.500	37.812	7.707634	0.2340
A $^1\Sigma_u^+$							
This work	1.0459	146 545	19230.9451	1835.355	33.3948	7.70235	0.1959
CEPA[a]	1.0457		19324.0742	1846.330	33.78		
MCSCF[b]	1.0457		19453.4843	1848.10	34.20	7.7030	0.2155
MCSCF/CI[c]	1.0440	146 120	19804	1860.30			
Experiment[d]	1.0406	146 365	19911.6660	1861.330	35.28	7.7789	0.2166
Experiment[e]	1.0404					7.78140	0.2197
b $^3\Pi_g$							
This work	1.0691	149 171	19403.3921	1752.968	36.1291	7.37337	0.2168
CEPA[a]	1.0689		19341.5621	1756.07	33.22		
MCSCF/CI[c]	1.0681	148 943	19947	1767.8			
Experiment[d]	1.0635	148 835	20250.9303	1769.07	35.02	7.4473	0.2196
Experiment[e]	1.0645			1769.337	35.249	7.433442	0.2191
B $^1\Pi_g$							
This work	1.0686	150 351	20271.9157	1752.974	36.7169	7.37848	0.2337
CEPA[a]	1.0726		20355.8574	1744.76	32.59		
MCSCF/CI[c]	1.0710	150 012	20925	1764.3			
Experiment[d]	1.0667	149 914	21219.7572	1765.76	34.39	7.4030	0.2160
Experiment[d]	1.0672			1766.151	34.586	7.39548	0.2156
c $^3\Sigma_g^+$							
This work.	1.0974	155 183	4158.6107	1565.288	54.0724	6.99713	0.3052
CEPA[a]	1.0980		4015.2103	1644.85	35.04		
MCSCF[b]	1.1004		4606.2997	1582.60	52.50	6.9322	0.2560
MCSCF/CI[c]	1.1030	154 703	4858	1589.5			
Experiment[d]	1.0966	155 053	4802.1636	1583.85	52.74	7.0048	0.3105
Experiment[e]	1.0977			1588.338	54.1555	6.99002	0.2638
C $^1\Sigma_g^+$							
This work	1.0930	157 669	8680.9674	1654.643	47.1574	7.05286	0.2489
CEPA[a]	1.0970		8380.1777	1652.43	28.74		
MCSCF[b]	1.0941		8729.9347	1652.90	40.40	7.0202	0.2300
MCSCF/CI[c]	1.0960	157 108	8819	1655.6			
Experiment[d]	1.0929	157 415	8862.8424	1653.43	41.04	7.0520	0.2150
Experiment[e]	1.0915			1571.809		7.07067	0.2472
F $^1\Pi_u$							
This work	1.0876	165 718	4905.3480	1662.426	43.1725	7.25258	0.2353
Experiment[d]	1.0849	165 971	5162.4133	1670.57	40.03	7.1560	0.2350
f $^3\Pi_u$							
This work	1.0891	166 669	2875.0025	1626.023	46.3226	7.10291	0.2482
Experiment[d]	1.0865	165 877	3207.2717	1661.48	44.79	7.1360	0.2281

[a] CEPA calculations of Wasilewski *et al.*[35].
[b] MCSCF calculations of Sunil *et al.* [19].
[c] MCSCF/CI calculations of Yarkony [21].
[d] Experiment from Huber and Herzberg [9].
[e] Experiments of Focsa *et al.* [1]

and CEPA-PNO and PNO-CI calculations of Wasilewski *et al.* [35] for the range of bond lengths considered in the present calculations. Figures 1 and 2 also compare calculations performed in this work with experimental results of Sprecher *et al.* [36] for the lowest four $np\sigma\,^3\Sigma_g^+$ and $np\sigma\,^3\Pi_g$ Rydberg states of He_2. These figures show that there are some similarity between our potential curves and those of Sprecher *et al.* [36] but not complete agreement. The slight differences observed can be accounted for by the difference in approach. A more informative method of considering the Rydberg states as a function of inter-nuclear distance R is to look at quantum defects as a function of R. Figures 3 and 4 show our effective quantum number of He_2 for singlet and triplet bound states, respectively. It can be seen that the effective quantum numbers show a weak dependence on the internuclear separation. Our methodology in essence is designed to determine quantum defects and can be expected to give approximately constant errors with respect to quantum defects rather than absolute or excitation energies. This means that the accuracy with which the binding energy of higher-lying states is determined in our calculations should improve as n increases.

From our calculated potential energy curves, the analytical potential energy functions of singlet $A^1\Sigma_g^+$, $B^1\Pi_g$, $C\,^1\Sigma_u^+$, $F^1\Pi_u$ and triplet $a^3\Sigma_u^+$, $b^3\Pi_g$, $c^3\Sigma_g^+$, $f\,^3\Pi_u$ Rydberg states of He_2 were fitted with Murrell-Sorbie(MS) [37] potential energy functions. The spectroscopic constants of each states are calculated through the relationship between analytical potential energy function and the spectroscopic constants [38]. Calculated spectroscopic constants are listed in Table 5 and compared with experimental results of Focsa *et al.* [1], Huber and Herzberg [9] and theoretical results obtained by Yarkony [21] and Wasilewski *et al.* [35]. It can be seen that our calculated T_e are very close to the experimental results of Sprecher *et al.* [36]. The other spectroscopic parameters are generally in agreement with the experiment and other theoretical works but that we can obtain results with the same level of accuracy for all observed states and, indeed, many more.

4. Conclusions

We have studied electron collisions with the He_2^+ molecular ion using UK R-Matrix molecular codes. Potential energy curves and quantum defects for singlet and triplet Rydberg states have been calculated as a function of internuclear separation. Our vertical excitation energies at 2.00 are in good agreement with the experiment. Spectroscopic constants of singlet $A^1\Sigma_g^+$, $B\,^1\Pi_g$, $C\,^1\Sigma_u^+$, $F\,^1\Pi_u$ and triplet $a\,^3\Sigma_u^+$, $b\,^3\Pi_g$, $c\,^3\Sigma_g^+$, $f\,^3\Pi_u$ Rydberg states of

He_2 are determined in the present work are in agreement with the experimental data and others theoretical calculations. The data presented in this work and the previous one [24], when combined, provide relevant parameters needed to calculate cross-section of DR and related processes of He_2.

ORCID

Jonathan Tennyson http://orcid.org/0000-0002-4994-5238

References

[1] C. Focsa, P.F. Bernath and R. Colin, J. Mol. Spectrosc. **191**, 209–214 (1998). doi:10.1006/jmsp.1998.7637

[2] J. van de Bovenkamp and J. van Duijneveldt, J. Chem. Phys. **110**, 11141–11151 (1999). doi:10.1063/1.479057

[3] T. van Mourik and T.H. Dunning, J. Chem. Phys. **111**, 9248–9258 (1999). doi:10.1063/1.479839

[4] S.M. Cybulski, Toczylowski, J. Chem. Phys. **111**, 10520–10528 (1999). doi:10.1063/1.480430

[5] R.J. Gdanitz, Molec. Phys. **99**, 923–930 (2001). doi:10.1080/00268970010020609

[6] A.J.C. Varandas, Theor. Chem. Acc. **119**, 511–521 (2010). doi:10.1007/s00214-008-0419-6

[7] I. Ema, G. Ramirez, R. Lopez and J.M.G. de la Vega, Computation **10**, 65–3197 (2022). doi:10.3390/computation10050065

[8] J.S. Cohen, Phys. Rev. A. **13**, 86–98 (1976). doi:10.1103/PhysRevA.13.86

[9] K.P. Huber and G. Herzberg, in *Molecular spectra and Molecular Structure: Vol 4. Constants of Diatomic Molecules*, (New York:Van Nostrand-Reinhold, 1979).

[10] A. Valance, S. Runge and Z. Physik, At. Mol. Clusters **10**, 483–490 (1999). doi:10.1007/BF01425767

[11] I. Hazell, A. Norregaard and N. Bjerre, J. Molec. Spectrosc. **172**, 135–152 (1995). doi:10.1006/jmsp.1995.1162

[12] B.J. Garrison, W.H. Miller and H.F. Schaefer, J. Chem. Phys. **59**, 3193–3198 (1973). doi:10.1063/1.1680460

[13] J. Komasa, Mol. Phys. **104**, 2193–2202 (2006). doi:10.1080/00268970600659461

[14] W.F. Curtis, Proc. R. Soc. London **89**, 146 (1913).

[15] F. Goldstein, Verh. Dtsch. Phys. Ges. **15**, 402 (1913).

[16] J.C. Browne, J. Chem. Phys. **42**, 2826–2829 (1965). doi:10.1063/1.1703246

[17] M.L. Ginter and R. Battino, J. Chem. Phys. **52**, 4469–4474 (1970). doi:10.1063/1.1673675

[18] S. Mukamel and U. kaldor, Molec. Phys. **22**, 1107–1117 (1971). doi:10.1080/00268977100103411

[19] K.K. Sunil, J. Lin, H. Siddiqui, P.E. Siska, K.D. Jordan and R. Shepard, J. Chem. Phys. **78**, 6190–6202 (1983). doi:10.1063/1.444583

[20] D.D. Konowalow and B.H. Lengsfield, J. Chem. Phys. **87**, 4000–4007 (1965). doi:10.1063/1.452903

[21] D.R. Yarkony, J. Chem. Phys. **90**, 7164–7175 (1989). doi:10.1063/1.456246

[22] B.M. McLaughlin, C.J. Gilan, P.G. Burke and J.S. Dahler, Phys. Rev. A. **47**, 1967–1980 (1993). doi:10.1103/PhysRevA.47.1967

[23] S.L. Guberman, in *Physics of Ion-Ion and Electron-ion Collision*, edited by F. Brouillard and J.W. McGowan (Plenum Press, New York and London, 1983), Vol. 167.

[24] M.D. Epée Epée, O. Motapon, D. Darby-Lewis and J. Tennyson, J. Phys. B: At. Mol. Opt. Phys. **50**, 115203 (2017). doi:10.1088/1361-6455/aa6a34

[25] B.K. Sarpal, S.E. Branchett, J. Tennyson and L.A. Morgan, J. Phys. B: At. Mol. Opt. Phys. **24**, 3685–3699 (1991). doi:10.1088/0953-4075/24/17/006

[26] D.A. Little and J. Tennyson, J. Phys. B: At. Mol. Opt. Phys. **46**, 145102 (2013). doi:10.1088/0953-4075/46/14/145102

[27] J. Tennyson, Phys. Rep. **491**, 29–76 (2010). doi:10.1016/j.physrep.2010.02.001

[28] J.M. Carr, P.G. Galiatsatos, J.D. Gorfinkiel, A.G. Harvey, M.A. Lysaght, D. Madden, Z. Mašín, M. Plummer, J.

[29] P.G. Burke, *R-Matrix Theory of Atomic Collisions: Application to Atomic, Molecular and Optical Processes* (Springer-Verlag, Berlin, 1965).

[30] J. Tennyson, J. Phys. B: At. Mol. Opt. Phys. **29**, 1817–1828 (1996). doi:10.1088/0953-4075/29/9/024

[31] A. Faure, J.D. Gorfinkiel, L.A. Morgan and J. Tennyson, Comput. Phys. Commun. **144**, 224–241 (2002). doi:10.1016/S0010-4655(02)00141-8

[32] C.J. Noble and R.K. Nesbet, Comput. Phys. Commun. **33**, 399–411 (1984). doi:10.1016/0010-4655(84)90145-0

[33] R. Zhang, K.L. Baluja, J. Franz and J. Tennyson, J. Phys. B: At. Mol. Opt. Phys. **44**, 035203 (2011). doi:10.1088/0953-4075/44/3/035203

[34] I. Rabadán and J. Tennyson, J. Phys. B: At. Mol. Opt. Phys. **29**, 3747–3761 (1996). doi:10.1088/0953-4075/29/16/018

[35] J. Wasilewski, V. Staemmler and R. Jaquet, Theoret. Chem. Acta. **59**, 517–526 (2010). doi:10.1007/BF00938693

[36] D. Sprecher, J. Liu, T. Krähenmann, M. Schäfer and F. Merkt, J. Chem. Phys. **140**, 064304 (2014). doi:10.1063/1.4364002

[37] J.N. Murrell and K.S. Sorbie, J. Chem. Soc. Faraday Trans **70**, 1552–1556 (1974). doi:10.1039/f29747001552

[38] C.-L. Yang, Y.-J. Huang and K.-L. Han, J. Mol. Struc. (THEOCHEM) **625**, 289–293 (2003). doi:10.1016/S0166-1280(03)00031-9

Tennyson and H.N. Varambhia, Eur. Phys. J. D. **66**, 58 (2012). doi:10.1140/epjd/e2011-20653-6